Porosity Cut-Off	Equivalent Hydrocarbon Column
0	423
0.02	423
0.05	423
0.08	423
0.1	423
0.13	423
0.14	421
0.15	420
0.17	407
0.2	382
0.25	272
0.3	113
0.35	20
0.37	4
0.4	1.75
0.45	0

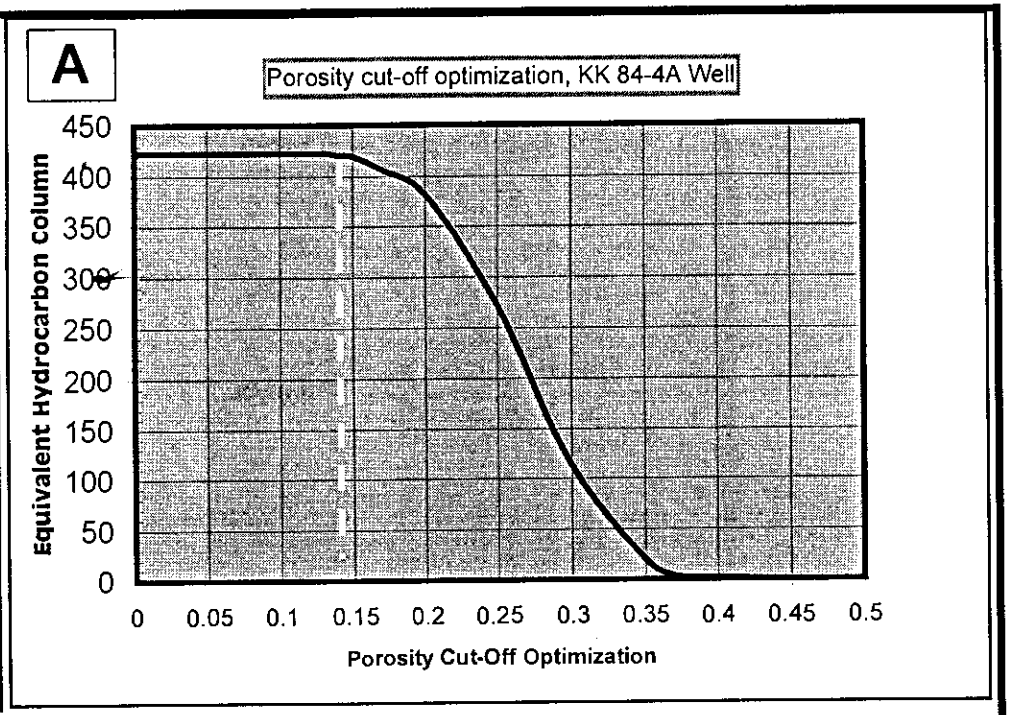

Sw Cut-Off	Equivalent Hydrocarbon Column
1	446.5
0.9	443.5
0.8	441
0.7	432
0.65	423
0.6	405
0.55	388
0.52	370
0.51	365
0.5	360
0.4	214
0.3	60
0.2	6
0.1	0
0	0

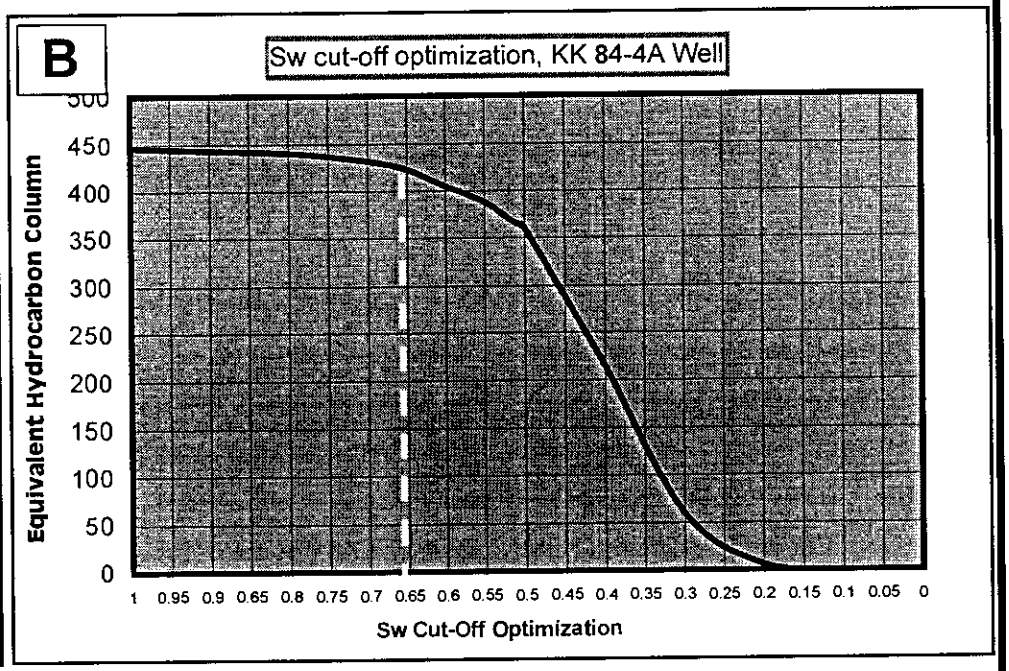

Fig. 28 : (A) - Porosity cut-off optimization.
(B) - Water saturation cut-off optimization.
KK 84-4A well, Nullipore rocks.

Porosity Cut-Off	Equivalent Hydrocarbon Column
0	430.5
0.06	430.5
0.1	430.5
0.12	430.5
0.14	430.5
0.145	430
0.15	429.5
0.17	428.5
0.18	427.5
0.2	426.5
0.22	418
0.26	367.5
0.28	286
0.3	218.5
0.32	163.5
0.36	65
0.4	12.5
0.43	1
0.44	0

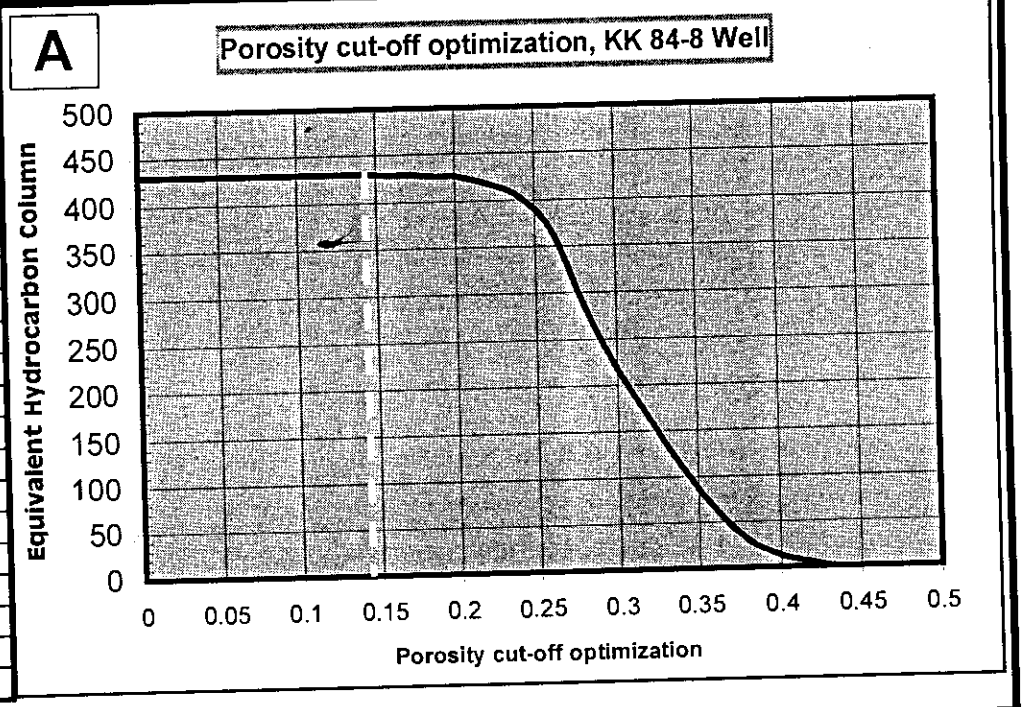

Sw Cut-Off	Equivalent Hydrocarbon Column
1	430.5
0.95	430.5
0.85	430.5
0.8	430.5
0.7	430.5
0.65	430.5
0.64	430
0.62	429
0.6	425
0.5	383
0.4	350
0.3	325
0.2	259
0.1	71
0.05	9
0.03	0

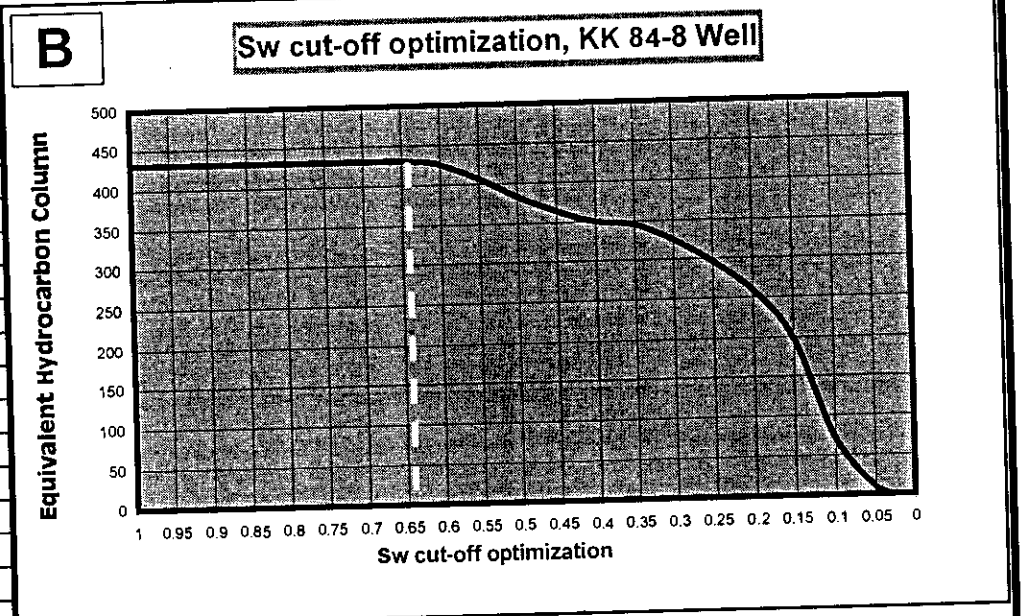

Fig. 29 : (A) - Porosity cut-off optimization.
(B) - Water saturation cut-off optimization.
KK 84-8 well, Nullipore rocks.

In most cases the hydrocarbon saturation and porosity cut-offs are synonymous in terms of identifying reservoir quality rock *(Keeplinger, 1981)*. Therefore, net oil pay has been defined as intervals with:

1. Porosity $\geq 14\ \%$
2. Hydrocarbon saturation $\geq 36\ \%$ (water saturation $\leq 64\ \%$).

In this study, the Reservoir Summation (ResSum) module (under Geoframe 404_Sun) is used to compute the reservoir properties for each zone (see appendix-2).

Zone properties are calculated by applying user-defined cut-off sets to selected curve data and summing the log intervals, which pass the specified criteria at the following stages of the computation process:

- Gross
- Net Reservoir
- Net Bay

Individual reservoir is normally described by single-parameter values representative of their characteristics. The most common parameters required in Nullipore reservoir illustration are listed in (Table 5).

6.3 Representation of the Different Deduced Petrophysical Data

The different deduced petrophysical data using different well logging analyses were represented in two methds. The first is the veratical represntation where the different deduced petrophysical parameters were represented vertically with depth in a number of what is called litho-saturation crossplots or petrophysical data logs (PDL), while the seconed is the lateral representation, where a number of iso-parameteric distribution maps were constructed.

WELL	ZONE	INTERVAL				GROSS Ft MD	GROSS Ft TVD	POROSITY (%)				PIGN	Kh md	SUWI	NET RESERVOIR	NET PAY	N/G Ratio
		TOP Ft MD	BTM Ft MD	TOP Ft TVDss	BTM Ft TVDss			ΦD	ΦN	ΦS	Φeff						
KK 84 - 1	ZONE I	2074	2265	2044	2235	191	191	0.26	0.25	0.22	0.255	0.25	1840	0.29	187.25	186.25	0.98
	ZONE II	2265	2438	2235	2408	173	173	0.3	0.28	0.24	0.29	0.29	5014	0.38	171.00	171.00	1.00
	ZONE III	2438	2770	2408	2740	332	332	0.26	0.24	0.21	0.25	0.26	212	0.58	124.00	9.25	0.07
KK 84 - 11	ZONE I	1986	2144	1822	1963	158	141	0.18	0.19	0.17	0.185	0.2	500	0.34	144.25	139.25	0.88
	ZONE II	2144	2380	1963	2174	236	211	0.22	0.24	0.2	0.23	0.23	304	0.32	234.50	229.00	0.97
	ZONE III	2380	3210	2174	2919	830	745	0.16	0.19	0.15	.17.5	0.17	4	0.49	266.00	188.00	0.45
KK 84 - 12	ZONE I	2322	2564	2197	2435	242	238	0.23	0.25	0.22	0.24	0.21	600	0.35	238.00	168.75	0.70
	ZONE II	2564	2768	2435	2636	204	200	0.26	0.29	0.28	0.27	0.27	740	0.55	30.00	17.00	0.08
	ZONE III	2768	3116	2636	2978	348	342	0.26	0.26	0.25	0.26	0.27	100	0.80	40.00	10.00	0.03
KK 84 - 8 (RF-B1)	ZONE I	2158	2334	2068	2244	176	176	0.24	0.28	0.24	0.26	0.25	2250	0.14	164.25	164.25	1.00
	ZONE II	2334	2514	2244	2424	180	180	0.31	0.31	0.3	0.31	0.29	4135	0.17	180.00	180.00	1.00
	ZONE III	2514	2692	2424	2602	178	178	0.28	0.32	0.28	0.3	0.31	1688	0.51	125.00	120.00	0.67
KK 84 - 4A	ZONE I	1987	2161	1955	2129	174	174	0.26	0.27	0.25	0.265	0.25	434	0.32	174.00	173.75	1.00
	ZONE II	2161	2339	2129	2307	178	178	0.23	0.25	0.2	0.24	0.24	638	0.34	178.00	178.00	1.00
	ZONE III	2339	2970	2307	2938	631	631	0.21	0.26	0.21	0.235	0.24	176	0.51	255.00	106.00	0.17
RF - A2	ZONE I	2527	2762	2153	2335	235	182	0.24	0.26	0.23	0.25	0.24	300	0.30	199.25	199.25	0.98
	ZONE II	-	-	-	-	-	-	-	-	-	-	-	-	-	-	-	-
	ZONE III	-	-	-	-	-	-	-	-	-	-	-	-	-	-	-	-
RF - A3	ZONE I	2558	2724	2219	2359	166	140	0.22	0.24	0.22	0.23	0.24	877	0.32	138.25	131.75	0.79
	ZONE II	-	-	-	-	-	-	-	-	-	-	-	-	-	-	-	-
	ZONE III	-	-	-	-	-	-	-	-	-	-	-	-	-	-	-	-
RF - B2	ZONE I	2519	2810	2059	2188	291	129	0.26	0.27	0.25	0.265	0.26	3886	0.14	251.75	249.25	0.86
	ZONE II	-	-	-	-	-	-	-	-	-	-	-	-	-	-	-	-
	ZONE III	-	-	-	-	-	-	-	-	-	-	-	-	-	-	-	-
RF - B3	ZONE I	2297	2521	2011	2170	224	159	0.24	0.28	0.25	0.26	0.26	1500	0.30	219.25	218.25	0.97
	ZONE II	2521	2640	2170	2256	119	86	0.23	0.24	0.23	0.235	0.24	1677	0.42	112.25	112.25	0.94
	ZONE III	-	-	-	-	-	-	-	-	-	-	-	-	-	-	-	-

ABBREVIATIONS

GROSS : Total thickness of reservoir rock (ft)

ΦD : Density derived porosity (%)

ΦN : Neutron derived porosity (%)

ΦS : Sonic derived porosity (%)

Φeff : Effective porosity (%)

PIGN : Intergranular porosity computed by ELANPlus program (%)

Kh : Log derived permeability (md)

SUWI : Water saturation computed by ELANPlus program (%)

NET RESERVOIR : Effective thickness after 14 % porosity cut-off (ft)

NET PAY : Effective thickness after 14 % porosity and 64 % water saturation cut-offs (ft)

N/G RATIO : Net pay/Gross ratio

Table (5) : Summary of petrophysical data results, Nullipore rock, Ras Fanar area.

6.3.1 Vertical Representation (Petrophysical Data Logs)

The petrophysical data log (PDL) is the final layout, which collects the different deduced petrophysical parameters, of prime interest, together and allows their interpretation vertically with depth.

Based on well logging and core samples analyses, its found that the petrophysical characteristics of Nullipore rocks in the different studied wells, are nearly similar to large extent with some relative differences in the percentages of the lithological components, pore spaces and fluid content. The petrophysical data logs of the different studied wells are constructed and represented in Appendix (1). In all data logs, water saturation increases with depth and hydrocarbon content is represented only by oil. Only one exception is found in KK84-11 well where some saturations of secondary gases are detected. In this part, we will deal with the petrophysical data logs of only two wells as examples, one is chosed as representative for the oil-bearing wells (KK84-4A), while the other well is only one where gases were recorded (KK84-11 well).

Fig. (30) shows the petrophysical data log of KK84-4A well. It indicates that the lithology of Nullipore reservoir is uniform and mainly dolomitic in composition. The pore spaces range between 22% to 30% and exhibit regular distribution allover the Nullipore section with some remarked increasing in the uppermost and lowermost parts. The fluid content is mainly water and hydrocarbon. Downgoing, water saturation (43%) shows general trend of increasing, therefore hydrocarbons are concentrated in the middle and upper parts of Nullipore rock. The oil-water contact in this well is found to be at depth 2434 ft.

(Fig. 30)

KK 84- 4a well

Petrophysical Data Log of Nullipore rocks

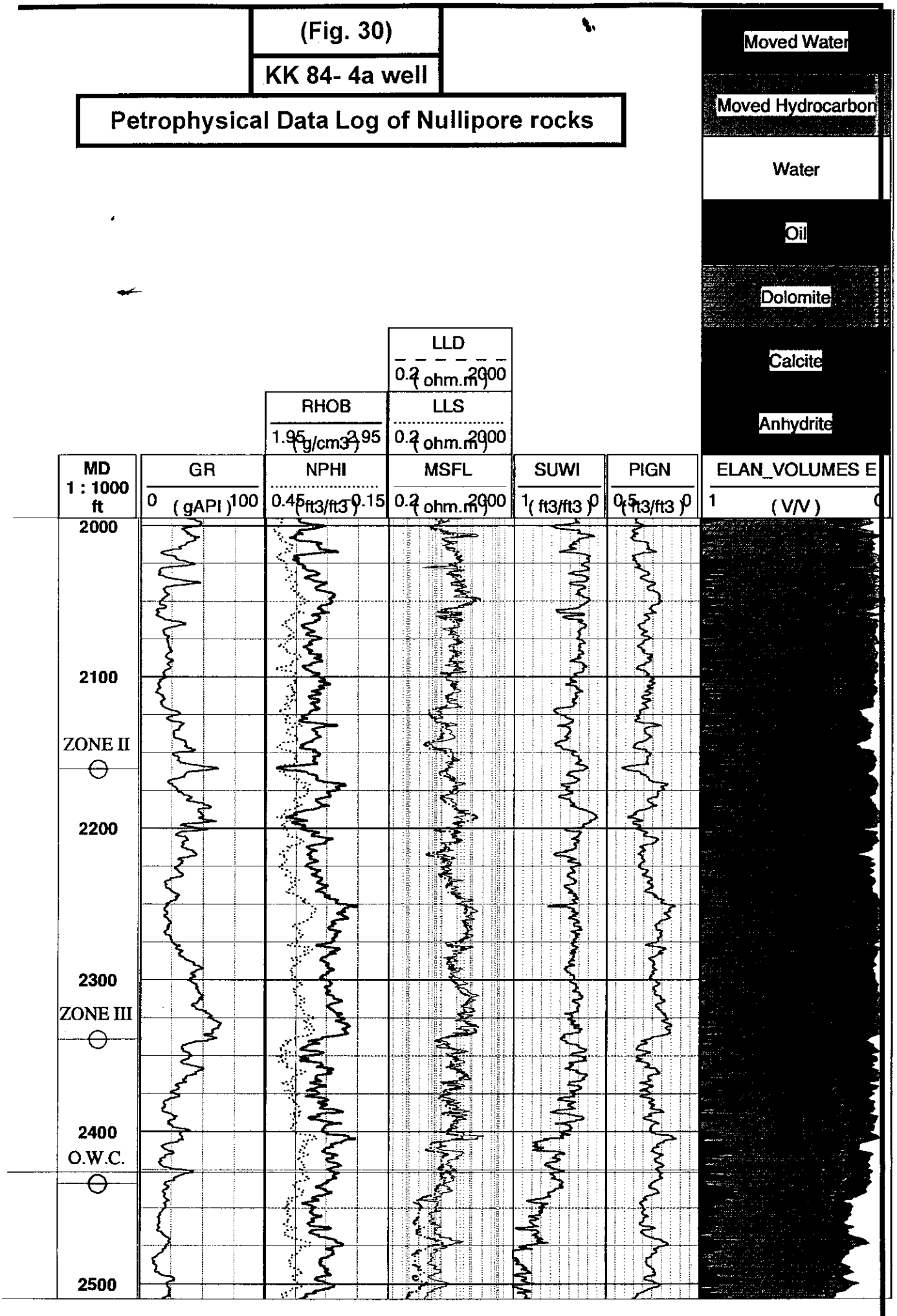

The petrophysical data log of KK84-11 well, on the other hand, is represented in Fig. (31). Like in KK84-4A well, the lithological content is mainly dolomite, with little percent of limestone lithology. The pore spaces are uniform allover the whole section except in the upper and lower parts (unlike KK84-4A well) of the rock. They range from 17% (zone III) to 23% (zone II). Water saturation increases remarkably in the lowermost parts of the rock. An average water saturation value of 37% is given for Nullipore rocks in this well. Hydrocarbon content is represented by oil with some saturations of secondary gases in zone (I) and uppermost part of zone (II). Depth of 2185 ft is considered the gas-oil contact in this well.

6.3.2 Lateral Distribution of Petrophysical Parameters

As previously mentioned, Ras Fanar field is an elongated horst block trending NW-SE direction, bounded by east and west clysmic faults. The geometry of the different petrophysical parameters was controlled by the geological position of the Nullipore reservoir rock.

Lateral distribution of these parameters was also enhanced in the present study, especially those parameters concerning with the hydrocarbon potentialities. In this respect a number of distribution maps were constructed for Nullipore reservoir such as porosity, water and hydrocarbon saturation maps.

6.3.2.1 Porosity Distribution Maps

Porosity distribution maps for Nullipore zones I, II and III were constructed (Figs. 32, 33 and 34). These maps show that one low porosity semi-closure between another two high porosity lobes (A and B lobes) can be recognized in all zones. This low porosity semi-closure is found in the

central part of the map, in the area between RF-A4 and RF-B3 wells. It attains the lowest porosity distributions allover the study area. Porosity values are found in increasing order to the northwest (A lobe) and southeast (B lobe) directions. These directions represent the highest porosity distributions among the study area.

The porosity distribution map of zone II (Fig. 33) attains much higher porosity values than in zones I and III. Maximum porosity value of 31 % is detected in the porosity distribution map of zone III (Fig. 34). It is recorded in KK 84-8 (RF-B1) well and represents the highest porosity closure in the field (B lobe).

In general, B lobe (RF-B2, RF-B3, KK 84-8, KK 84-1, KK 84-11 and KK 84-12 wells) attains higher porosity and better reservoir quality than A lobe (RF-A2, RF-A3, and KK 84-4A wells).

6.3.2.2 Water Saturation Distribution Map

Water saturation map of Nullipore reservoir rock is represented in Fig. (35). It appears clearly that water saturation increases in the eastern and western boundaries of the field. Upgoing, the water saturation values decrease to the central part along the northwest-southeast axis.

Two low water saturation closures are found in the study area. They are represented by (A) lobe in northwestern part and (B) lobe in the southeastern part of the field. The minimum water saturation is observed at the central part of (B) lobe and represented by RF-B2 well (Sw = 15 %). Menwhile, maximum values of 45 % and 43 % are recorded in KK 84-12 and KK 84-4A wells, respectively.

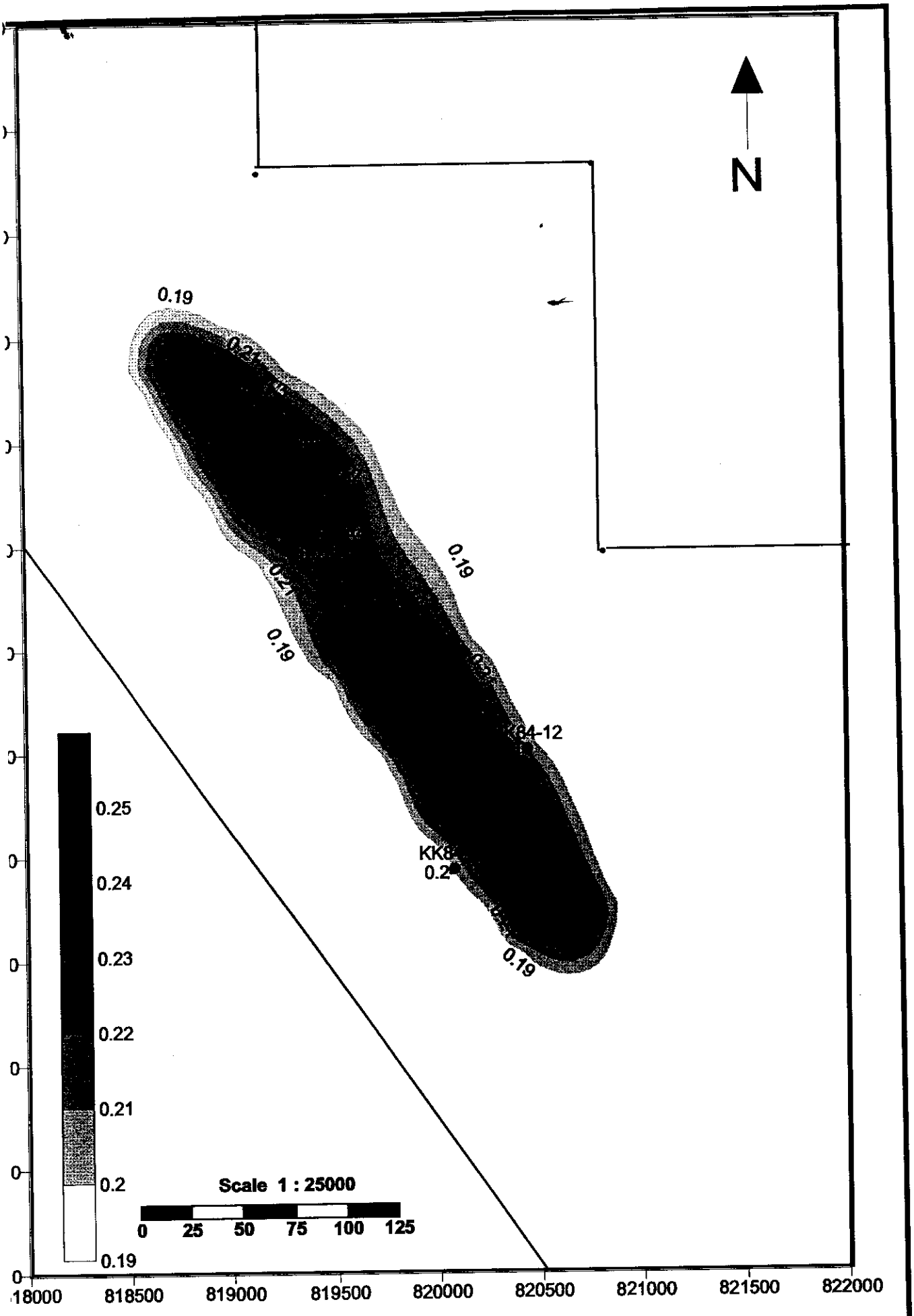

Fig. 32 : ZONE (I) Porosity distribution map, Nullipore rocks, Ras Fanar field.

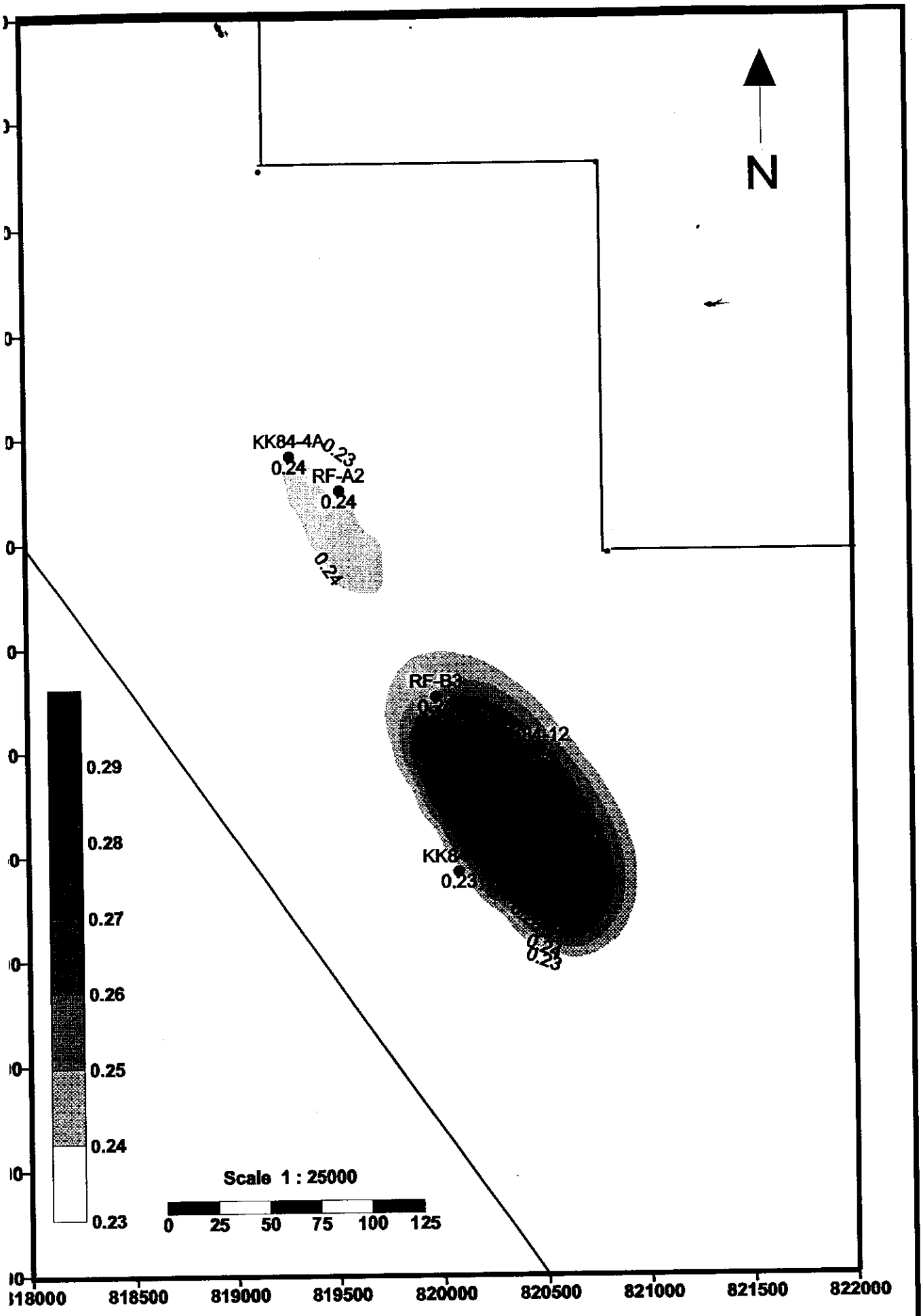

Fig. 33 : ZONE (II) Porosity distribution map, Nullipore rocks, Ras Fanar field.

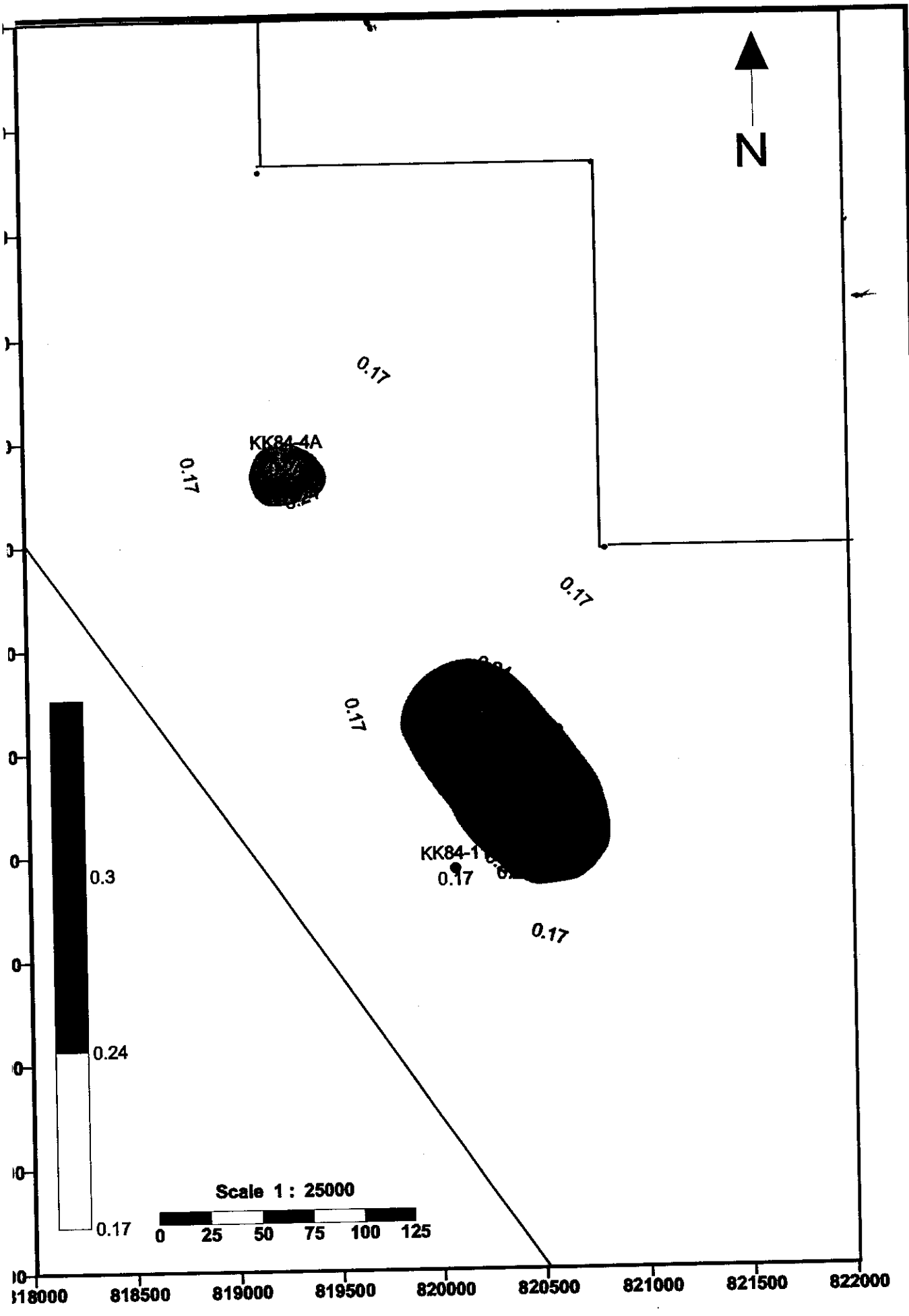

Fig. 34 : ZONE (III) Porosity distribution map, Nullipore rocks, Ras Fanar field.

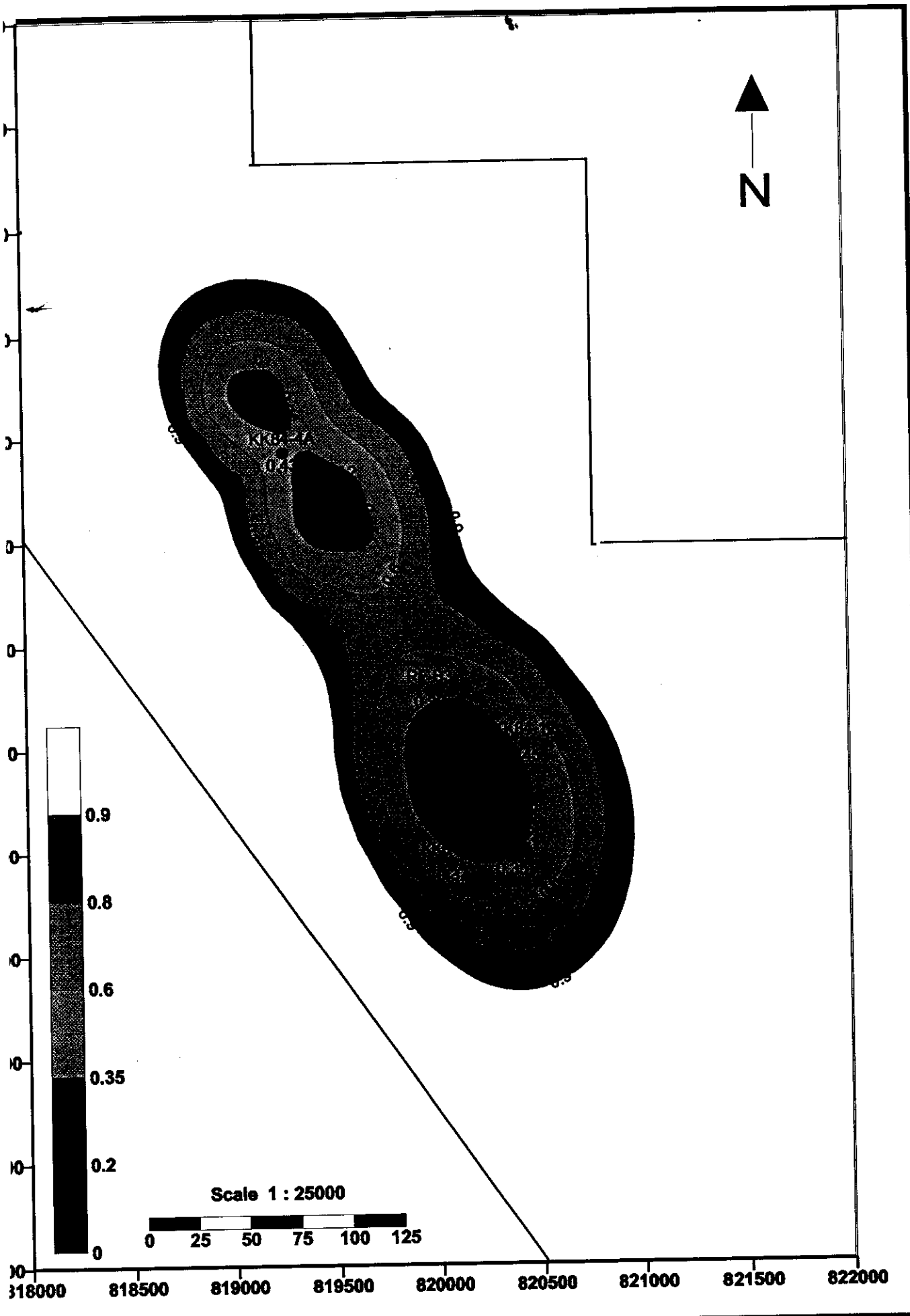

Fig. 35 : Water saturation map of Nullipore rocks, Ras Fanar field.

6.3.2.3 Hydrocarbon Saturation Distribution Map

Fig. (36) shows the hydrocarbon saturation distribution map of Nullipore reservoir. The map illustrates that hydrocarbon saturation increases remarkably inside the two lobes (A and B)

The maximum hydrocarbon saturation (85 %) was recorded in RF-B2 well, while the minimum saturation (55 %) was detected in KK 84-12 well.

6.4 Nullipore Reservoir Quality Distribution

Porosity, water and hydrocarbon saturation maps of Nullipore reservoir show that the best reservoir quality is found at the central parts of (B) and (A) lobes. The reservoir quality decreases gradually towards the northwest and southeast directions, almost elongated as well as the general trend of the Ras Fanar horst block. They also indicate that the reservoir quality decreases rapidly towards the east and west directions, controlled by the east and west bounding faults.

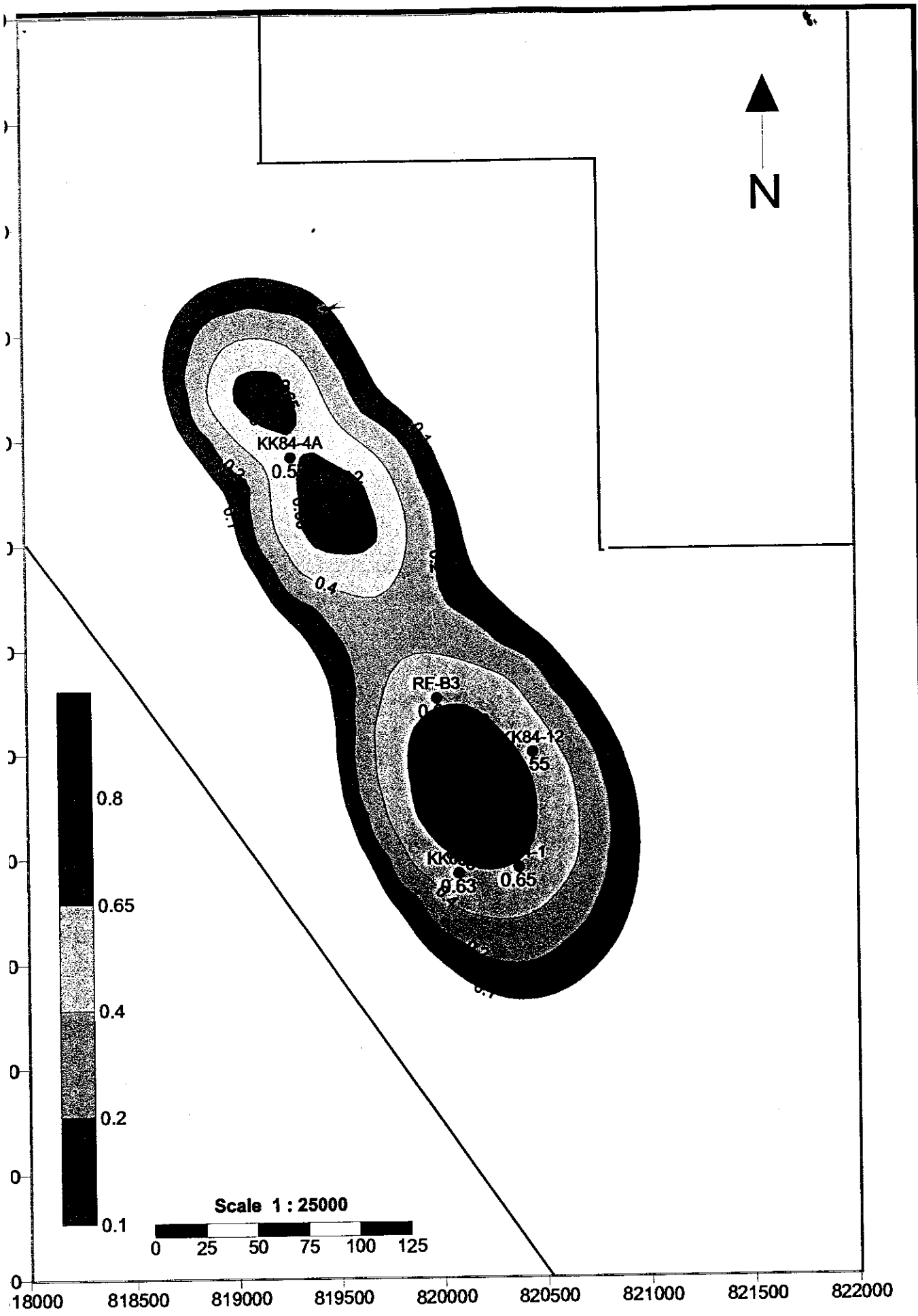

Fig. 36 : Hydrocarbon saturation map of Nullipore rocks, Ras Fanar field.